

# Epitaxial growth of gallium nitride thin films on A-plane sapphire by molecular beam epitaxy

D. Doppalapudi,<sup>a)</sup> E. Iliopoulos, S. N. Basu, and T. D. Moustakas

Center for Photonics Research, College of Engineering, Boston University, Boston, Massachusetts 02215

(Received 12 October 1998; accepted for publication 23 December 1998)

In this article, we propose a crystallographic model to describe epitaxy of GaN on  $(11\bar{2}0)$  sapphire (A plane). The  $(1\bar{1}02)$  cleavage plane in sapphire is shown to extend to the GaN lattice as the  $(11\bar{2}0)$  plane, facilitating the formation of cleaved facets. It is shown that, although the lattice mismatch is much smaller than in the case of epitaxy on (0001), the difference in the planar symmetry in this case results in high-strained bonds near the interface. The use of nitridation and a low temperature buffer is therefore necessary. A systematic study of GaN growth on the A-plane sapphire by plasma-assisted molecular beam epitaxy was carried out to study the effects of plasma nitridation of the substrate and the growth of a low temperature GaN buffer on the structure and optoelectronic properties of the films. Transmission electron microscopy (TEM) studies indicate that films grown on substrates which were not nitridated prior to growth have a significant fraction of zinc-blende domains and poor orientation relationship with the substrate. On the contrary, nitridation leads to films with superior structural and optoelectronic properties. The low temperature GaN buffer, grown on nitridated substrates, was found to also have a pronounced effect on the optoelectronic properties of the GaN films, especially in those with low carrier concentrations. The correlation between TEM and photoluminescence studies suggests that the transition at 3.27 eV can be attributed to the cubic domains in the films. © 1999 American Institute of Physics. [S0021-8979(99)02507-4]

## I. INTRODUCTION

The lack of good quality GaN substrates led to investigation into several different substrates for epitaxial growth of GaN, of which, C-plane (0001) sapphire is the most widely studied substrate. Due to the large lattice mismatch ( $\sim 14\%$ ), several approaches have been adapted to optimize the nucleation and growth of GaN layers on these substrates. Amano *et al.*<sup>1</sup> found that high-quality nitride films can be grown by metalorganic vapor phase epitaxy on C-plane sapphire by forming an initial thin AlN buffer layer at low temperature. Moustakas *et al.*<sup>2,3</sup> and Nakamura<sup>4</sup> have shown that a low temperature GaN buffer layer also improves the epitaxial growth of GaN by molecular beam epitaxy (MBE) and metalorganic chemical vapor deposition techniques, respectively. The Boston University group has also demonstrated that the conversion of the surface of  $\text{Al}_2\text{O}_3$  to AlN by exposure to a nitrogen plasma leads to improvements in the subsequent epitaxial growth.<sup>2,5</sup> Since then, other groups have reported similar benefit upon nitridation of the sapphire substrate by exposure to ammonia.<sup>6-8</sup> Recently, energetics of AlN thin films on sapphire surface have been calculated and shown that AlN (and the GaN film grown on it) can have different polarities, depending on the nucleation conditions.<sup>9</sup> The AlN thin film that formed upon nitridation was found to be oriented such that it is rotated  $30^\circ$  in-plane with respect to the substrate lattice:  $(0001)_{\text{AlN}} \parallel (0001)_{\text{sapphire}}$  and  $[10\bar{1}0]_{\text{AlN}} \parallel [11\bar{2}0]_{\text{sapphire}}$ .<sup>7,10,11</sup> Subsequent growth of GaN

is in the same orientation as AlN. The presence of AlN with  $30^\circ$  rotation reduces the mismatch between the substrate and the epitaxial layer and thus also reduces the strain in the layer. However, the absence of a good cleavage plane perpendicular to the C plane of sapphire makes it difficult to form cleaved surfaces, which are required to form edge-emitting lasers.

III-nitride films grown on  $(11\bar{2}0)$  sapphire (A plane) can be cleaved more easily along R plane, to form edge-emitting lasers. In addition, since the lattice mismatch between GaN and A-plane sapphire is less than 2%,<sup>12</sup> it is expected that better quality films may be achieved. The Boston University group has shown that GaN films grown on A-plane sapphire with initial nitridation and low temperature GaN buffer layers were smoother than those grown on C-plane sapphire by a similar method.<sup>2,3</sup> In these studies, the preferred epitaxial orientation relationship was found to be  $(0001)_{\text{GaN}} \parallel (11\bar{2}0)_{\text{sapphire}}$  and  $[10\bar{1}0]_{\text{GaN}} \parallel [10\bar{1}0]_{\text{sapphire}}$ . There have also been some studies on the effect of GaN and AlN buffer layers on the growth of GaN on A-plane sapphire.<sup>13</sup> Kato *et al.* have reported that the GaN films they deposited on A-plane sapphire had mixed orientations; they observed GaN with (0001) and  $(10\bar{1}0)$  orientations parallel to  $(11\bar{2}0)$  sapphire.<sup>14,15</sup> However, there have been no systematic studies of how the nitridation of the A-plane sapphire affects the epitaxial growth and properties of the overgrown GaN films.

In this article, a crystallographic model has been developed to study the epitaxy of GaN over  $(11\bar{2}0)$  sapphire.

<sup>a)</sup>Electronic mail: dharani@engc.bu.edu

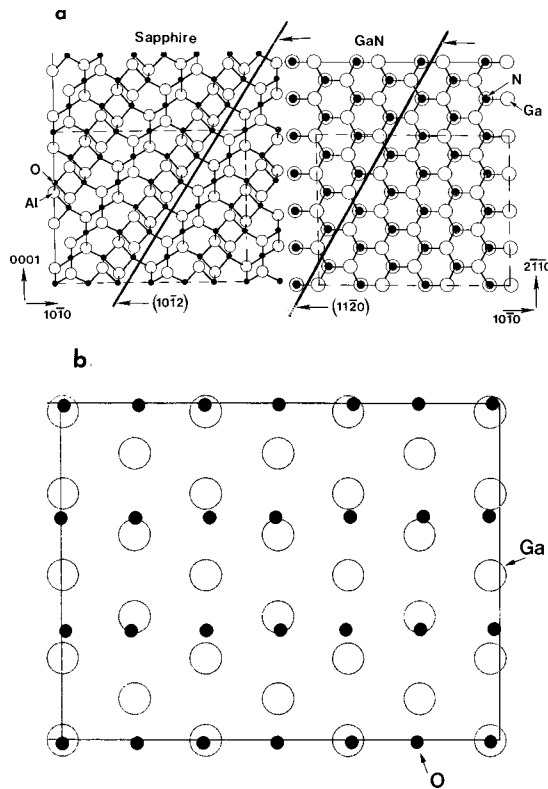


FIG. 1. Projections of sapphire and GaN lattices (a)  $(11\bar{2}0)$  and  $(0001)$  planes of sapphire and GaN respectively, showing the cleavage planes. The rectangles depict the supercells of overlap. (b) A supercell of GaN  $(0001)$  epitaxy on sapphire  $(1120)$ .

Epitaxial growth on this plane has been investigated by MBE.

## II. CRYSTALLOGRAPHIC MODEL

Crystallographic modeling of the interface is a very useful tool to understand the issues of epitaxy. Researchers at Northwestern University have described crystallographic models of  $(0001)$  AlN thin films on  $(0001)$  and  $(01\bar{1}2)$  faces of sapphire.<sup>16,17</sup> Sapphire belongs to space group  $R\bar{3}c = D_3^6d$  (No. 167) and the crystal structure can be described as  $O^{2-}$  anions in approximately hexagonal-close-packed arrangement, with  $Al^{3+}$  cations occupying two-thirds of the octahedral voids. A detailed description of the structure is given by Kronberg.<sup>18</sup> GaN with wurtzite structure (hexagonal symmetry) belongs to space group  $P6_3Mc$  (No. 186). As seen in the x ray and transmission electron diffraction studies, epitaxial GaN grows with the  $(0001)$  plane parallel to the  $(11\bar{2}0)$  plane of sapphire. However, the epitaxy is not straightforward, since the epitaxial plane of GaN does not share the same symmetry as that of sapphire.

As mentioned in the introduction, one of the major advantages of A-plane sapphire is the presence of the cleavage plane perpendicular to the sapphire surface. The cleavage plane in the sapphire crystal is  $(10\bar{1}2)$  (*R* plane), which is the close-packed plane (interplanar spacing of 3.48 Å). Figure 1(a) shows  $20 \times 20$  Å crystallographic projections of  $(11\bar{2}0)$  and  $(0001)$  planes of sapphire and GaN, respectively, simulated using the Crystal Kit program.<sup>19</sup> The projections of the

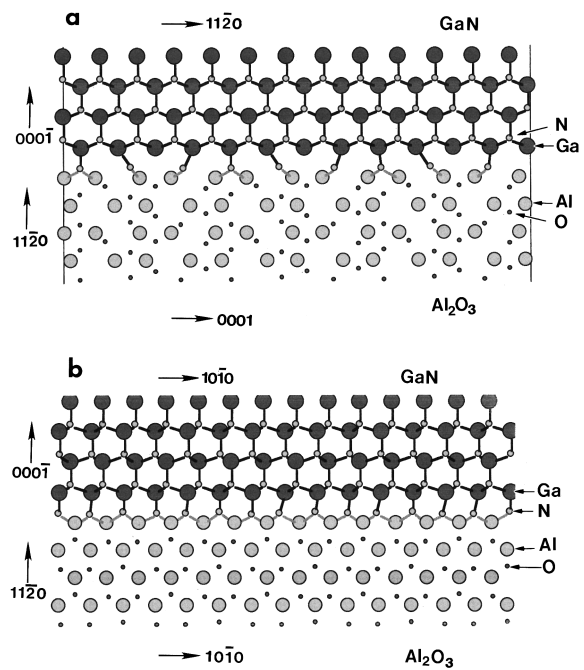


FIG. 2. Crystallographic model of cross-sectional view of the interface, seen at (a)  $[1\bar{1}00]_{GaN}$  zone-axis and (b)  $[11\bar{2}0]_{GaN}$  zone-axis.

cleavage planes in the two lattices are marked in Figure 1(a). The line in sapphire is the projection of  $(10\bar{1}2)$  plane (*R* plane), which is shown to be approximately parallel to the projection of  $(11\bar{2}0)$  plane in GaN. However, it should be noted that there is  $2.4^\circ$  rotation in between these two cleavage axes across the interface. The supercell of epitaxial overlap is outlined by the dotted rectangles ( $\sim 13 \times 16.5$  Å) in the two projections. Figure 1(b) shows superimposition of the two projections. The thickness in the *z* direction is restricted to a monolayer in each lattice, to include only the atoms closest to the interface that participate in the chemical bond.

Figure 2 is a schematic of the cross-section of the sapphire/GaN interface showing the bonding across the interface. Figure 2(a) is the cross-section at the  $[1\bar{1}00]$  zone-axis in GaN (which is equivalent to the  $[1\bar{1}00]$  zone-axis in sapphire), and Fig. 2(b) is the cross-section at the  $[11\bar{2}0]$  zone-axis in GaN ( $[0001]$  zone-axis of sapphire). The cross-section is taken from the line of best match, i.e., the edges of the supercell outlined by a rectangle in Fig. 1. In these two models, a *z* range of 2 Å is taken to simplify the picture, and the same kind of lattice matching is assumed as in Fig. 1(b). As seen in the projection, GaN is shown to be growing with a  $[000\bar{1}]$  polarity (Ga to N bond pointing down), which is consistent with our experimental reflection high-energy electron diffraction (RHEED) observations described later.

The supercell of epitaxial overlap is outlined by the rectangles in the two projections in Fig. 1(a). With this supercell, the lattice match is as follows: six  $(10\bar{1}0)$  planes of GaN match with four planes of  $(10\bar{1}0)$  of sapphire, resulting in a lattice mismatch of  $-0.62\%$ . In the perpendicular direction, eight planes of  $(11\bar{2}0)$  GaN match with one  $(0001)$  plane of sapphire, resulting in a mismatch of 1.8%. Based on the above projections, the expected distances between misfit dislocations are 179 and 443 Å in  $[11\bar{2}0]$  and  $[1\bar{1}00]$  directions

of GaN, respectively. This is in contrast to GaN growth on (0001) sapphire, where the lattice mismatch is 14% and misfit dislocations are expected every 36 Å. Based on these models, we see that the lattice mismatch between the GaN and sapphire supercells is significantly smaller than the corresponding mismatch on (0001) sapphire. This raises the question whether the nitridation and low temperature GaN buffer steps, which were shown to lead to high quality GaN films on (0001) sapphire, are necessary in this case. However, as can be seen in the projections, a large fraction of the atomic bonds in the supercell are highly distorted across the interface and do not match perfectly with the GaN structure, resulting in a strained GaN film. Therefore, a nucleation step may be required for growth on *A* plane as well.

It is known that the sapphire lattice is terminated by oxygen atoms at the surface. This presence of oxygen species at the interface can complicate the epitaxy of GaN, by formation of GaO layer at the interface. Exposure of the *A*-plane sapphire to a nitrogen plasma results in replacement of all the O atoms on the surface by N thereby forming a monolayer of strained AlN. We believe that this facilitates the subsequent growth of GaN on a better (chemically) matched substrate. In Fig. 2, the top monolayer of "O" atoms in sapphire are shown to be replaced by "N" atoms.

### III. EXPERIMENTAL DETAILS

GaN films were grown by MBE using a Varian Gen II system, as described previously.<sup>3,5</sup> Active nitrogen was produced by passing 10 sccm molecular nitrogen through an ASTeX compact electron cyclotron resonance (ECR) source, producing a downstream pressure of  $10^{-5}$  to  $10^{-4}$  Torr. Pre-cleaned *A*-plane sapphire substrates were outgassed in the buffer chamber at 600 °C before loading in to the growth chamber. A number of films were grown directly on the sapphire substrate at 775 °C, without nitridation or low temperature buffer. Several films were also grown on nitridated sapphire, by heating the substrates to 750 °C and exposing to a 150 W nitrogen microwave plasma for different time intervals. GaN buffer layers (when used) were grown at 550 °C to a thickness of about 20–30 nm. All the films discussed in this report were doped *n* type with Si, by varying the temperature of the Si effusion cell between 1000 and 1200 °C.

The structural quality of the samples was studied *in situ* by RHEED, and by scanning electron microscopy (SEM), atomic force microscopy (AFM), x-ray diffraction (XRD), and TEM techniques after the growth. XRD studies were performed using a four-circle diffractometer with  $\text{CuK}\alpha$  radiation as the excitation source. Cross-sectional TEM samples were prepared by "sandwiching," mechanical thinning, dimpling, and ion-milling to electron transparency. The TEM and high resolution electron microscopy (HREM) studies were carried out using a JEOL 2000FX and a JEOL 3000FX electron microscope, respectively. AFM analysis was carried out with a Digital Instruments scanning probe, operated in tapping mode. The optical and transport properties of the films were determined by measuring the photoluminescence (PL) spectra and the Hall effect (using the Van der Paw method), respectively. PL in the films was excited

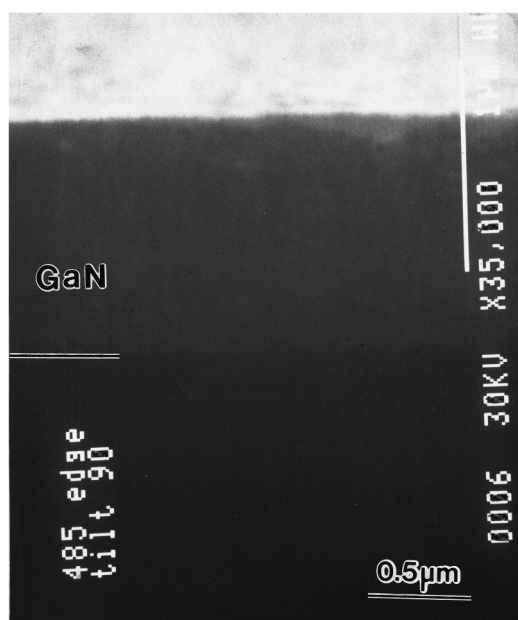


FIG. 3. SEM micrograph of the cleavage facet near the GaN sapphire interface.

with a 10 mW He–Cd laser (325 nm wavelength) and the spectra were dispersed with a 0.5 m spectrometer equipped with a holographic grating blazed at 250 nm and detected with a photomultiplier. Hall effect measurements were done on cloverleaf patterns that were lithographically etched on to  $5 \times 5$  mm samples using a Bio-rad pattern maker. Contacts on these *n*-type samples were made with indium dots soldered at the four points of the clover leaf shape. Hall measurements were taken at room temperature, by injecting  $10^{-6}$  to  $10^{-3}$  A current in the presence of a 7 KG magnetic field.

### IV. RESULTS AND DISCUSSION

As mentioned earlier, one of the major incentives for choosing *A*-plane sapphire is the ability to form cleaved facets. Figure 3 shows an SEM micrograph of a cleaved interface for a typical film, showing very smooth surfaces across the interface. The cleavage plane in sapphire corresponds to (1102) (*R* plane), which is the close packed plane (interplanar spacing of 3.48 Å) in this lattice. This *R* plane is perpendicular to the surface and has a orientation that is  $\sim 58^\circ$  from the [1100] direction in the surface plane of sapphire. The extension of this cleavage plane matches with the (11 $\bar{2}$ 0) plane in GaN, which is also a major crystallographic plane. In view of these results, we investigated the optimum growth conditions for the growth of GaN on *A*-plane sapphire.

#### A. Films grown without nitridation and low temperature GaN buffer

GaN films of approximately 1  $\mu\text{m}$  thickness were grown directly on the *A*-plane sapphire after thermal outgassing at 775 °C. In these films, cubic features were observed by RHEED during the early stages of growth, as shown in the Fig. 4. Based on the RHEED patterns from thick GaN films, the camera length of the diffraction system was calculated and used to estimate the interplanar spacing of the planes

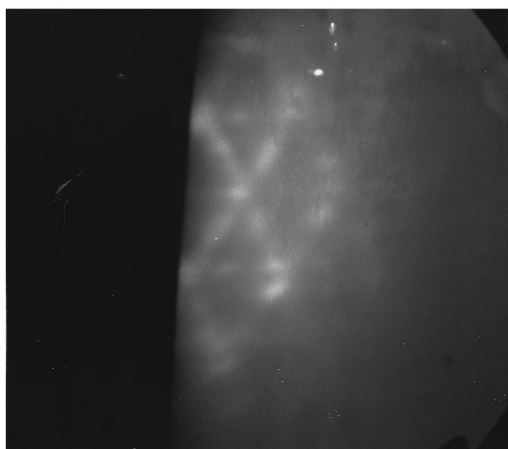


FIG. 4. RHEED pattern from GaN film grown directly on A-plane sapphire, viewed at  $[11\bar{2}0]_{\text{GaN}}$  zone-axis.

responsible for the pattern. Based on these calculations, it was determined that the pattern in Fig. 4 is a superimposition of RHEED from  $[11\bar{2}0]$  zone-axis of wurtzite GaN and  $[110]$  zone-axis of zinc-blende GaN. Although the films had predominantly wurtzite structure after further growth, they were defective. This was also observed in the TEM studies, as described later. Figure 5 is a cross-sectional TEM micrograph of a GaN film, showing that the film is indeed polycrystalline and polymorphic. The inset electron diffraction pattern, taken from the region of sapphire/GaN interface, shows an overlap of the diffraction patterns from sapphire and GaN. It is clear from the absence of matching between the diffraction spots, that there is no specific epitaxial relationship between the grown film and the substrate. Regions of zinc-blende phase were clearly observed in electron diffraction analysis and are marked by arrows in the figure. It is known that GaN can exist both in wurtzite and zinc blende structures<sup>20</sup> and that the cohesive energies of the two structures are comparable.<sup>3</sup> Thus, optimization of the growth parameters, especially in the initial nucleation stages is very important to obtain GaN in the desired phase. In view of

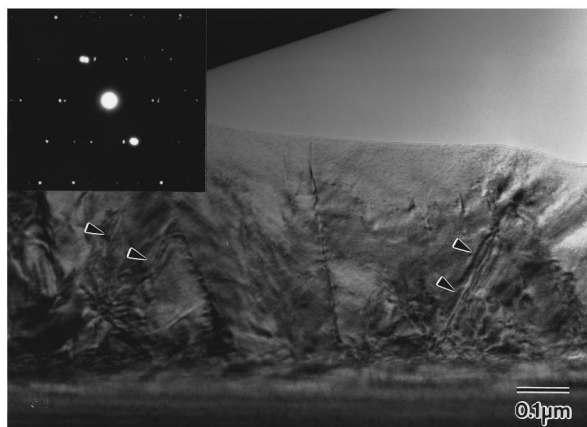


FIG. 5. Cross-sectional TEM micrograph of a GaN film grown without nitridation or low temperature buffer; the inset electron diffraction shows the absence of a clear epitaxial relation between the film and the substrate.

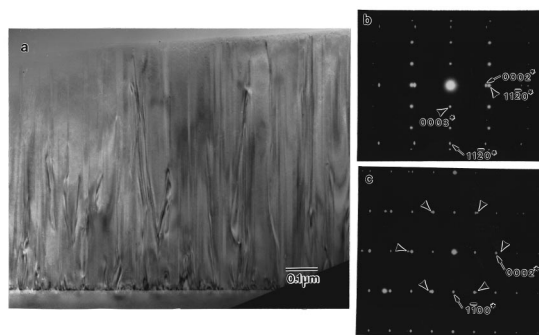


FIG. 6. (a) Cross-sectional TEM micrograph of a GaN film grown after nucleation by nitridation and a low temperature buffer. Excellent match between reciprocal lattice points of GaN (arrows) and sapphire (triangles) is seen, as shown from the electron diffraction patterns from the film interface (b) near  $[10\bar{1}0]$  zone-axis of GaN (and  $[10\bar{1}0]$  zone-axis of sapphire), and (c) near  $[11\bar{2}0]$  zone-axis of GaN (also  $[0001]$  zone-axis of sapphire). The triangles in (c) represent the  $\{11\bar{2}0\}$  family of planes in the reciprocal space.

these findings, the effect of nitridation and low temperature GaN buffer on the properties of the films was explored.

## B. Films grown with low temperature GaN buffer and with/without nitridation

All the GaN films in this study had a 20 nm thick low temperature GaN buffer layer grown at  $550^\circ\text{C}$  and a  $1\ \mu\text{m}$  thick GaN film, grown at  $775^\circ\text{C}$ . Analyses of the GaN film grown without the nitridation step by RHEED and XRD indicated that the film was polycrystalline. Cross-sectional TEM showed that the film is polycrystalline and had structure similar to that shown in Fig. 5. XRD studies of the films grown on nitridated sapphire substrates showed that GaN grows with the (0002) plane parallel to the A plane of sapphire. The intensity and the full width at half maximum (FWHM) of the (0002) peak improved significantly with nitridation for these samples. The FWHM of the (0002) peak was  $\sim 110$  arc sec for the films on fully nitridated surface. The rocking curve at (0002) peak was typically around 600 arc sec for films with  $1\ \mu\text{m}$  thickness. Figure 6(a) is the cross-sectional TEM micrograph of GaN film grown after nitridating the substrate for 15 min. The film is single crystal GaN, with a defective buffer layer near the interface. Figure 6(b) is a selective area diffraction (SAD) pattern near  $[10\bar{1}0]$  zoneaxis (of both lattices) from the interface. It shows that in reciprocal space,  $(11\bar{2}0)_{\text{sapphire}}^*$  is parallel to  $(0002)_{\text{GaN}}^*$  and  $(0003)_{\text{sapphire}}^*$  is parallel to  $(11\bar{2}0)_{\text{GaN}}^*$ . The lattice mismatch can be estimated from the separation of these reciprocal lattice points. Figure 6(c) is a SAD pattern from the  $[11\bar{2}0]$  zone-axis of GaN (or  $[0001]$  zone-axis of sapphire), also showing a good epitaxial orientation between the GaN film and sapphire. These results confirm that GaN epitaxy on A-plane sapphire occurs as:  $[11\bar{2}0]_{\text{GaN}} \parallel [0003]_{\text{sapphire}}$  and  $[0002]_{\text{GaN}} \parallel [11\bar{2}0]_{\text{sapphire}}$ . This is in agreement with the previous reports of epitaxial relation between GaN and A-plane sapphire.<sup>11,12</sup> In these films which resulted in smooth surfaces,  $1 \times 1$  reconstruction was observed during growth, which developed into  $3 \times 3$  reconstruction during cooling down, as shown in Fig. 7. Such reconstruction is an indication of predominantly N-terminated (or  $[000\bar{1}]$ ) polarity.<sup>21</sup>

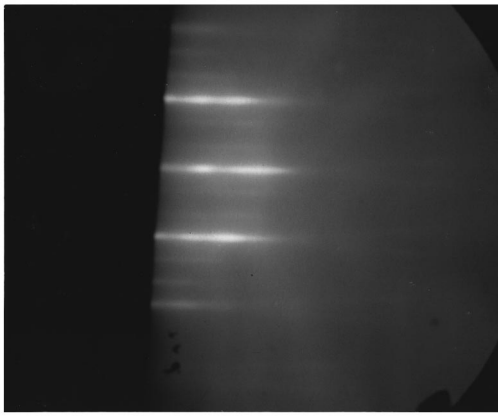


FIG. 7. RHEED pattern viewed at  $[11\bar{2}0]_{\text{GaN}}$  zone-axis, from GaN film grown after nitridation and buffer steps.

Convergent beam electron microscopy studies are being currently done to confirm this observation. Preliminary TEM studies show that there are still some domain boundaries. Though the density of threading dislocations is high ( $\sim 10^{10} \text{ cm}^{-2}$ ), no cubic domains and very few stacking faults were detected in TEM and HREM studies. These data clearly indicate the importance of the nitridation step of the A-plane sapphire for the epitaxial growth of GaN. This, we believe, is due to the formation of AlN nuclei on the surface of  $\text{Al}_2\text{O}_3$ , which promotes wetting and facilitates two-dimensional growth.

Nitridation also was found to have significant effect on the surface roughness and transport properties in such films. Table I summarizes these data in three of the GaN films grown with increasing nitridation times, keeping all other growth parameters identical. A clear improvement of surface morphology was observed with increase in nitridation time, as indicated by root mean square (rms) roughness values measured by AFM. Figure 8 shows SEM micrographs of the three samples taken under the same magnification. It is clear from the figure that there is a dramatic improvement in surface morphology with nitridation time. Sample I has a rough surface morphology, indicative of three-dimensional growth. Sample II has considerably smoother surface [as shown in Fig. 8(b)] as well as some rough regions (not shown in this micrograph), indicating insufficient nucleation of AlN on the surface. Sample III, which was grown on sapphire nitridated for 15 min has a very smooth, specular surface. This improvement in the morphology is consistent with the hypothesis that nitridation promotes wetting and thus two-dimensional growth.

TABLE I. The effect of nitridation on the physical properties of GaN films on A-plane sapphire.

Sample	Nitridation (min)	rms roughness (nm)	$n$ ( $\text{cm}^{-3}$ )	$\mu$ ( $\text{cm}^2/\text{Vs}$ )
I	0	40	$1.1 \times 10^{19}$	1
II	5	4	$9.8 \times 10^{18}$	89
III	15	1.5	$7 \times 10^{18}$	119

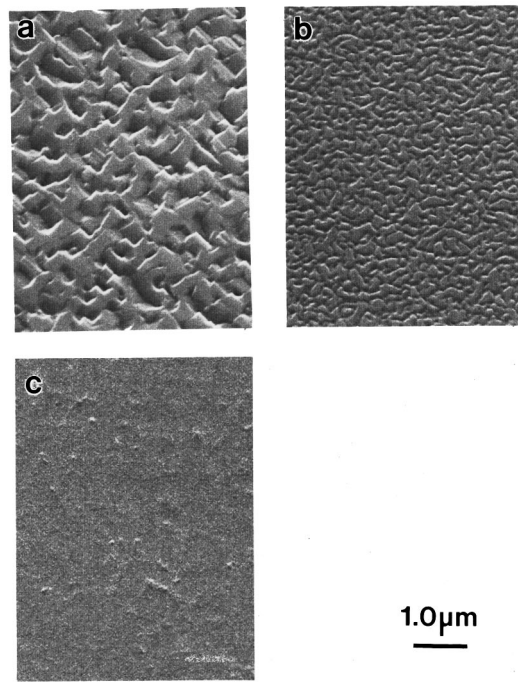


FIG. 8. SEM micrographs from 1 mm thick GaN films grown with (a) 0, (b) 5, and (c) 15 min nitridation.

Table I also summarizes the effect of nitridation on transport coefficients. While the doping level ( $\sim 1 \times 10^{19} \text{ cm}^{-3}$ ) did not change upon nitridation, the electron mobility improved by more than a factor of 100. This dramatic change is attributed to the polycrystalline nature of the films grown with no or poor nitridation. These mobility values of the order of about  $120 \text{ cm}^2/\text{V}$  for the films grown on the nitridated substrates are as high as those reported for GaN films grown by MBE on the C-plane sapphire at the same level of doping.<sup>22</sup> To the best of our knowledge, there are no reports on the mobility of GaN films at these doping levels on A-plane sapphire.

PL measurements were carried out at room temperature and at 77 K to investigate the effect of the substrate nitridation on the optical properties of the films. Figure 9 shows the PL spectra of the three samples described above, both at 300 K (dotted lines) and at 77 K (solid lines). At 300 K, the film grown on the surface without nitridation has a broad peak at 3.3 eV with a low energy tail, while samples II and III show the excitonic lines of wurtzite GaN at 3.4 eV, indicating that nitridation is essential to improve film properties. To reveal the differences between the films more clearly, PL measurements were done at 77 K (Fig. 9). Sample I, which was not nitridated, shows very a broad peak near 3.27 eV. Sample II, with 5 min nitridation, has the dominant peak at 3.27 eV with a weaker peak near 3.47 eV, associated with neutral donor bound exciton of wurtzite GaN. At the low energy side of the 3.27 eV peak, two other peaks at 3.19 and 3.11 eV could be resolved, which are the 1 and 2 longitudinal optical (LO) phonon replicas of the 3.27 eV transition, respectively. Finally, GaN film grown after 15 min nitridation has only one peak at 3.47 eV, with a FWHM of 45 meV. These data show the importance of optimization of the nitridation step to

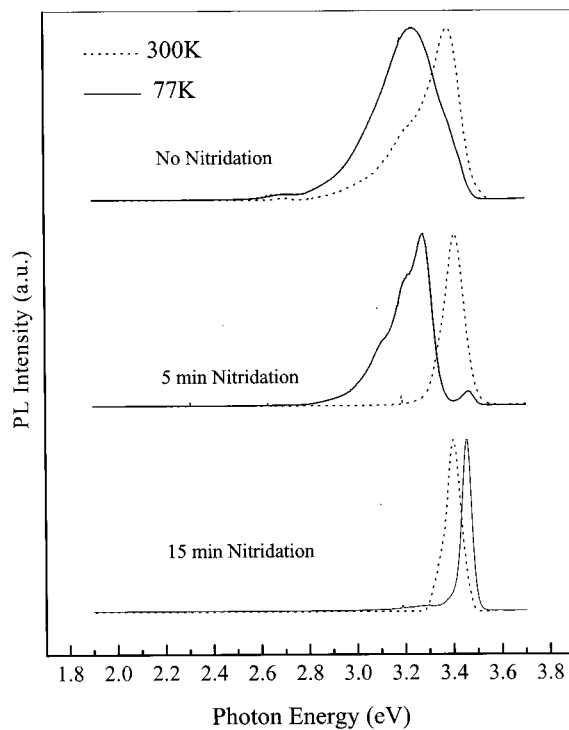


FIG. 9. PL spectra from GaN films with different nitridation times taken at 300 (dotted lines) and 77 K (solid lines).

obtain good GaN epitaxial films. The FWHM values quoted for the completely nitridated sample at 300 K (60 meV) and 77 K (45 meV) are comparable to the state-of-the-art for GaN samples with similar carrier concentration ( $\sim 10^{19} \text{ cm}^{-3}$ ). These values are also similar to the FWHM of Si-doped GaN films grown on C-plane sapphire with the same donor concentration.<sup>23</sup> This broadening is due to a combination of thermal broadening and potential fluctuations created by the random spatial distribution of impurity atoms in the host crystal and is consistent with the analysis of those fluctuations based on Morgan's impurity band broadening model.<sup>23</sup>

Several researchers have observed these transitions near 3.27 eV earlier.<sup>24–26</sup> While some researchers<sup>24,25</sup> attribute these peaks to donor-acceptor transitions in wurtzite GaN, Moustakas<sup>26</sup> proposed that this is a result of the zinc-blende domains or isolated stacking faults in the wurtzite structure. Such structural inhomogeneities give rise to potential fluctuations in the conduction band of about 0.2 eV, which is the difference in the band gap between wurtzite and zinc-blende GaN.<sup>26</sup> The direct correlation between the PL spectra and the cubic domains observed in the TEM studies strongly support the second hypothesis.

### C. Films grown with nitridation and with/without low temperature GaN buffer

The effect of low temperature GaN buffer on the film properties was studied in two sets of samples as listed in Table II. Samples A and B were doped heavily with Si and samples C and D were doped relatively less. In the samples A and B, the presence of buffer layer did not make a signifi-

TABLE II. The effect of low temperature buffer on the GaN film properties.

Sample	Buffer	Thickness ( $\mu\text{m}$ )	rms roughness (nm)	$n$ ( $\text{cm}^{-3}$ )	$\mu$ ( $\text{cm}^2/\text{Vs}$ )
A	0	0.9	8	$8.9 \times 10^{18}$	97
B	20 nm	1.0	2	$7 \times 10^{18}$	118
C	0	1.5	9	$2.7 \times 10^{17}$	135
D	20 nm	1.5	3	$3.5 \times 10^{17}$	211

cant difference in the structural quality of the resultant films, as observed in RHEED and TEM studies. Both films had comparable dislocation densities ( $\sim 8 \times 10^{10} \text{ cm}^{-2}$ ), as well as electron mobilities ( $\sim 100 \text{ cm}^2/\text{V sec}$ ). However, XRD results show that the sample grown without a buffer step is more compressively strained, as indicated by the increase in the  $c$  parameter. The  $c$  parameter is calculated to be 5.188 Å for the film grown on a low temperature buffer, compared to 5.1896 Å for the film grown without a buffer step. These observations were made *in situ* as well, from the RHEED patterns. It was observed that the epitaxial films were initially strained and relaxed as further deposition occurred. The films grown on low temperature buffers seem to relax very quickly, within the first 4–10 min of growth (equivalent of 10–25 nm). The films grown without a buffer, on the other hand, were found to be strained, sometimes even when the film thickness exceeded 1  $\mu\text{m}$ .

PL studies at 77 K showed that the GaN film grown with a buffer had a peak at 3.460 eV (corresponding to the donor bound excitons of wurtzite GaN) with a FWHM of 40 meV, as shown by the plot with solid line in Fig. 10. The GaN film grown without a buffer layer, on the other hand, had a broader peak at 3.465 eV, with a FWHM of 47 meV (dotted

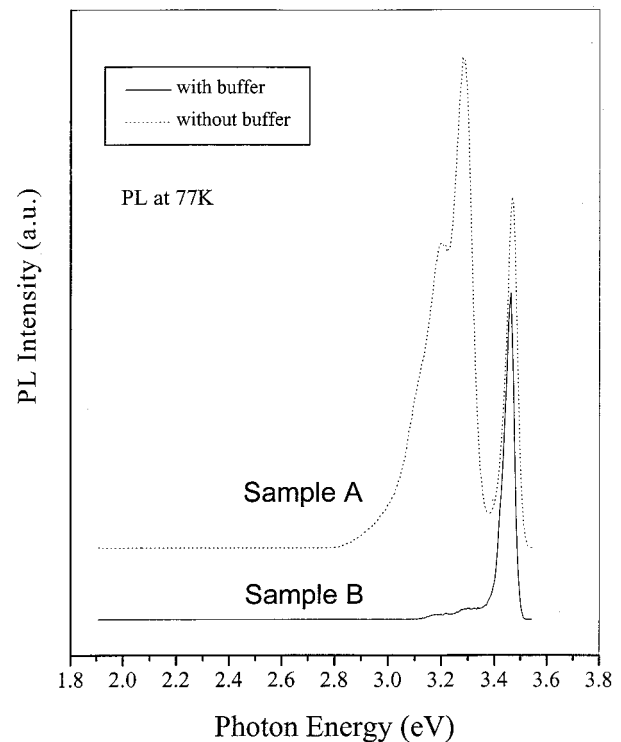


FIG. 10. PL spectra at 77 K from samples A and B.

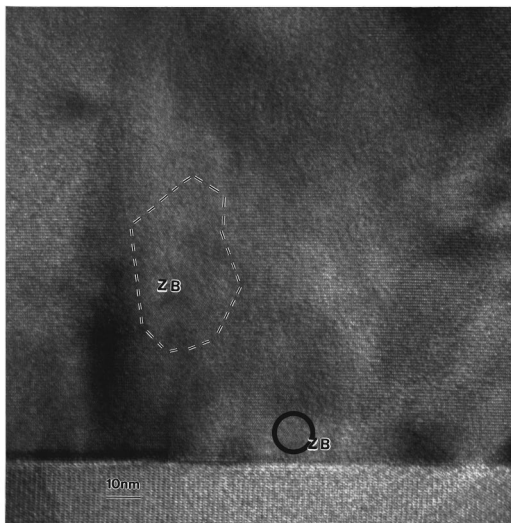


FIG. 11. HREM of sample A (grown without buffer). The cubic domains are indicated and marked as “ZB”.

line in Fig. 10). The blue-shift of 5 meV is consistent with the compressive stress observed in the film, as observed in RHEED and XRD studies. This indicates that the buffer layer results a partial relief of stresses in the films. Furthermore, the PL spectra from the films grown without a buffer layer had a strong secondary peak at 3.27 eV, with LO phonon replicas at 3.19 and 3.11 eV. As discussed earlier, this peak was attributed to cubic domains and/or isolated stacking faults. Figure 11 shows a high resolution electron micrograph of the sample A near the interface. Zinc-blende domains are clearly identified and are as large as 40 nm in some cases. We could not identify any such cubic domains in film B, which was grown on a low temperature buffer. This provides further support to our earlier correlation between the transition at 3.27 eV and the cubic features.

In the lightly doped films, the benefit of GaN buffer was more obvious. Specifically, the threading defects were predominantly inversion domains in the film without a buffer. The inversion domain boundary (IDB) density was observed to be a factor 5 higher in sample C, compared to sample D. This difference in the defect character is clearly shown by TEM micrographs in Fig. 12. Figure 12(a) is a bright field micrograph from sample C, showing predominantly domain boundaries (marked by arrows). On the other hand, Figure 12(b) shows a much smaller concentration of domain boundaries in sample D. This difference reflected in the transport properties of the films as well. The electron mobility in the film grown with a low temperature buffer is a factor of 2 higher than in the film without a buffer, as shown in Table II. This, we believe, is due to the piezo-electric effect of the different polarities in the samples. The quoted mobilities are lower than the best electron mobility in GaN grown on A plane of  $\sim 400$  reported by Doverspike *et al.*<sup>13</sup> Further optimization of the growth process is required to match these mobilities.

Figure 13 shows the PL spectra from samples C and D at 300 (dotted line) and at 77 K (solid line). The PL spectra at 77 K from these samples also show peaks at 3.27 eV, which

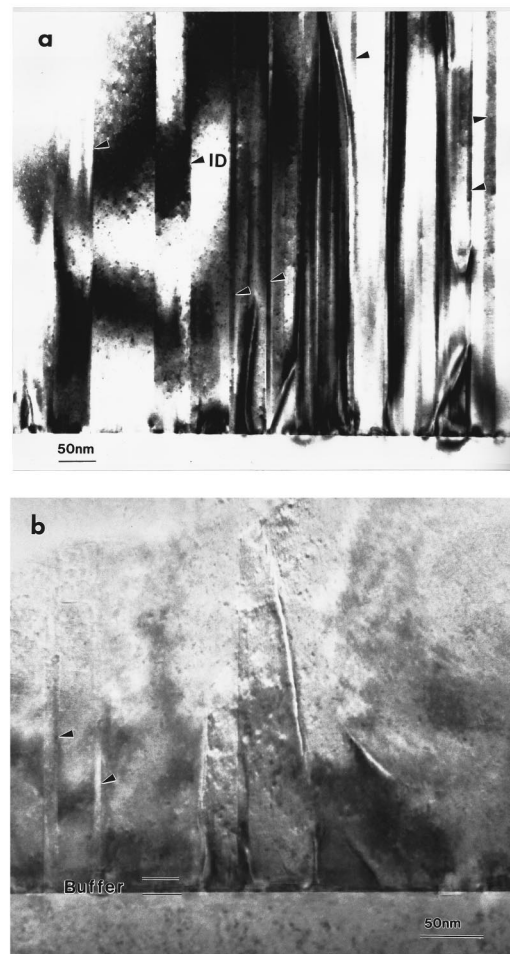


FIG. 12. TEM micrographs from sample C and D. The film grown without buffer layer shows predominantly domain boundaries (a), whereas the film grown on buffer has very few domain boundaries (b).

are not visible in the spectra taken at 300 K. The use of buffer dramatically reduced the PL features attributed to cubic domains. The FWHM of the peaks associated with the neutral donor bound excitons for sample D are 38–40 and 22 meV at 300 and 77 K, respectively. These values are similar to the state-of-the-art in GaN films with  $\sim 10^{17} \text{ cm}^{-3}$  carrier concentration and are very close to the values expected by the cumulative effect of thermal broadening (39 meV at 300 K and 10 meV at 77 K), static disorder and inhomogeneous strain.<sup>23</sup>

With above described optimized nucleation conditions on A-plane sapphire, GaN films were grown with a wide range of doping levels ( $< 10^{15}$  to  $> 10^{19} \text{ cm}^{-3}$ ) by varying the silicon effusion cell temperature. Undoped films with very smooth surface morphology were grown with resistivity of  $\sim 10^4 \Omega \text{ cm}$ . In such highly resistive samples, accurate measurement of carrier concentration is difficult, but we believe it is below  $10^{15} \text{ cm}^{-3}$ , since we can typically measure concentrations above that value. These resistive films also showed good PL near 3.415 eV (FWHM=46 meV) at 300 K.

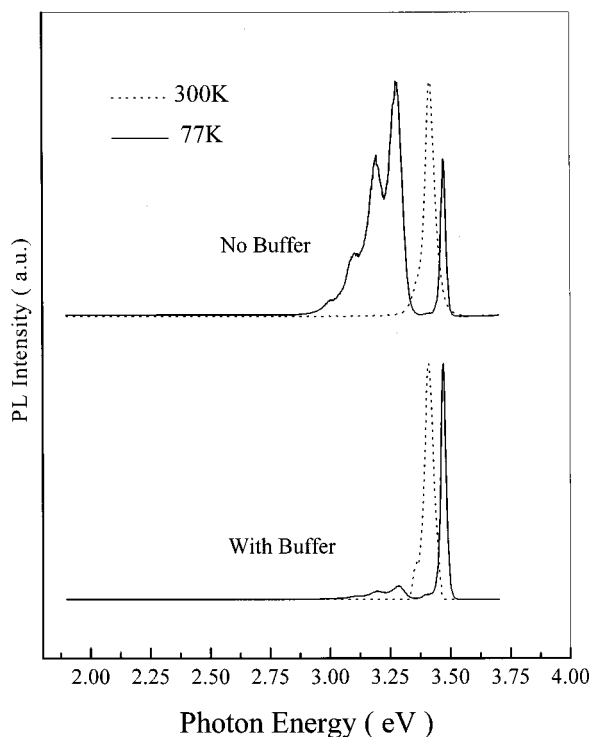


FIG. 13. PL spectra from samples C and D taken at 300 (dotted lines) and 77 K (solid lines).

## V. CONCLUSION

A crystallographic model was proposed to describe epitaxy of GaN on (11 $\bar{2}$ 0) sapphire. It is shown that, although the lattice mismatch is much smaller than in the case of epitaxy on (0001), the difference in the planar symmetry in this case results in highly strained bonds near the interface. Use of a low temperature buffer is therefore necessary. Nitridation step is believed to benefit the epitaxy by converting the top surface of sapphire (which is a poor quality crystal due to the polishing) to crystalline AlN. The cleavage plane in sapphire, (1 $\bar{1}$ 02), is shown to extend in to the GaN lattice as (11 $\bar{2}$ 0) plane, facilitating the formation of cleaved facets. Experimentally, the structure as well as the physical properties of GaN films grown on the A-plane sapphire were found to depend sensitively on nitridation of the substrate surface. Nitridation with an ECR nitrogen plasma (150 W at 750 °C) for about 10–15 min was found to lead to GaN films with good epitaxial relationship to the substrate and good luminescence and transport properties. The presence of a low

temperature buffer layer was found to affect the film properties favorably, especially in the films with low Si doping. The PL transitions at 3.27 eV observed in the films with out optimized nitridation or buffer were correlated with TEM studies and attributed to the cubic domains in the films.

## ACKNOWLEDGMENTS

The authors would like to thank Center for Electron Microscopy, MIT for the use of microscopy facility and Dr. Y. Fedyunin and A. Krupp for useful discussions. The Project was partially supported by the Office of Naval Research under Contract No. N00014-98-1-0213 (monitored by Dr. Colin Wood).

- <sup>1</sup>H. Amano, N. Sawaki, I. Akasaki, and Y. Toyoda, *Appl. Phys. Lett.* **48**, 353 (1986).
- <sup>2</sup>T. D. Moustakas, R. J. Molnar, T. Lei, G. Menon, and C. R. Eddy, Jr., *Mater. Res. Soc. Symp. Proc.* **242**, 427 (1992).
- <sup>3</sup>T. D. Moustakas, T. Lei, and R. J. Molnar, *Physica B* **185**, 36 (1993).
- <sup>4</sup>S. Nakamura, *Jpn. J. Appl. Phys., Part 2* **30**, L1705 (1991).
- <sup>5</sup>T. D. Moustakas and R. J. Molnar, *Mater. Res. Soc. Symp. Proc.* **281**, 753 (1993).
- <sup>6</sup>S. Keller, B. P. Keller, Y. F. Wu, B. Heying, D. Kapolnek, J. S. Speck, U. K. Mishra, and S. P. DenBaars, *Appl. Phys. Lett.* **68**, 1525 (1996).
- <sup>7</sup>N. Grandjean, J. Massies, and M. Leroux, *Appl. Phys. Lett.* **69**, 2071 (1996).
- <sup>8</sup>K. Uchida, A. Watanabe, F. Yano, M. Kouguchi, T. Tanaka, and S. Min-gawa, *J. Appl. Phys.* **79**, 3487 (1996).
- <sup>9</sup>R. Di Felice and J. E. Northrup, *Appl. Phys. Lett.* **73**, 936 (1998).
- <sup>10</sup>D. Korakakis, Ph.D. thesis, Boston University, 1998.
- <sup>11</sup>T. Lei, K. F. Ludwig Jr., and T. D. Moustakas, *J. Appl. Phys.* **74**, 4430 (1993).
- <sup>12</sup>T. Matsuoka, T. Sakai, and A. Katsui, *Optoelectron. Devices Technol.* **5**, 53 (1990).
- <sup>13</sup>K. Doverspike, L. B. Rowland, D. K. Gaskill, and J. A. Freitas, Jr., *J. Electron. Mater.* **24**, 269 (1994).
- <sup>14</sup>T. Kato, H. Ohsato, T. Okuda, P. Kung, A. Saxler, C. Sun, and M. Razeghi, *J. Cryst. Growth* **173**, 244 (1997).
- <sup>15</sup>T. Kato, P. Kung, A. Saxler, C. Sun, H. Ohsato, M. Razeghi, and T. Okuda, *Solid-State Electron.* **41**, 227 (1997).
- <sup>16</sup>C. J. Sun, P. Kung, A. Saxler, H. Ohsato, K. Haritos, and M. Razeghi, *J. Appl. Phys.* **75**, 3964 (1994).
- <sup>17</sup>P. Kung, C. J. Sun, A. Saxler, H. Ohsato, and M. Razeghi, *J. Appl. Phys.* **75**, 4515 (1994).
- <sup>18</sup>M. L. Kronberg, *Acta Metall.* **5**, 507 (1957).
- <sup>19</sup>Distributed by Total Resolution, Berkeley, CA.
- <sup>20</sup>S. Strite and H. Morkoc, *J. Vac. Sci. Technol. B* **10**, 1237 (1992).
- <sup>21</sup>A. R. Smith, R. M. Feenstra, D. W. Greve, M. S. Shin, M. Skowronski, J. Neugebauer, and J. E. Northrup, *Appl. Phys. Lett.* **72**, 2114 (1998).
- <sup>22</sup>N. G. Weimann, L. F. Eastman, D. Doppalapudi, H. M. Ng, and T. D. Moustakas, *J. Appl. Phys.* **83**, 3656 (1998).
- <sup>23</sup>E. Iliopoulos, D. Doppalapudi, H. M. Ng, and T. D. Moustakas, *Appl. Phys. Lett.* **73**, 375 (1998).
- <sup>24</sup>O. Lagerstedt and B. Monemar, *J. Appl. Phys.* **45**, 2266 (1979).
- <sup>25</sup>M. Ilegems and R. Dingle, *J. Appl. Phys.* **39**, 4234 (1973).
- <sup>26</sup>T. D. Moustakas, *Mater. Res. Soc. Symp. Proc.* **395**, 111 (1996).